REPORT

Cell Cycle 10:12, 2021-2034; June 15, 2011; © 2011 Landes Bioscience

Matrix remodeling stimulates stromal autophagy, "fueling" cancer cell mitochondrial metabolism and metastasis

Remedios Castello-Cros,[1,2,*] Gloria Bonuccelli,[1,2] Alex Molchansky,[1,2] Franco Capozza,[1,2] Agnieszka K. Witkiewicz,[1,3] Ruth C. Birbe,[1,3] Anthony Howell,[4] Richard G. Pestell,[1,2] Diana Whitaker-Menezes,[1,2] Federica Sotgia[1,2,4] and Michael P. Lisanti[1,2,4,5,*]

[1]The Jefferson Stem Cell Biology and Regenerative Medicine Center; [2]Departments of Stem Cell Biology and Regenerative Medicine and Cancer Biology; [3]Department of Pathology, Anatomy and Cell Biology; [5]Department of Medical Oncology; Kimmel Cancer Center; Thomas Jefferson University; Philadelphia, PA USA; [4]Manchester Breast Centre and Breakthrough Breast Cancer Research Unit; Paterson Institute for Cancer Research; School of Cancer; Enabling Sciences and Technology; Manchester Academic Health Science Centre; University of Manchester; Machester UK

Keywords: caveolin-1, plasminogen activator inhibitor, cancer-associated fibroblasts, autophagy, tumor stroma, apoptosis, breast cancer, metastasis

Abbreviations: Cav-1, caveolin-1; KO, knockout; WT, wild-type; MSFs, mammary stromal fibroblasts; PAI-1, plasminogen activator inhibitor type-1; PAI-2, plasminogen activator inhibitor type-2; uPA, urokinase-type plasminogen activator; CAFs, carcinoma-associated fibroblasts

We have previously demonstrated that loss of stromal caveolin-1 (Cav-1) in cancer-associated fibroblasts is a strong and independent predictor of poor clinical outcome in human breast cancer patients. However, the signaling mechanism(s) by which Cav-1 downregulation leads to this tumor-promoting microenvironment are not well understood. To address this issue, we performed an unbiased comparative proteomic analysis of wild-type (WT) and Cav-1$^{-/-}$ null mammary stromal fibroblasts (MSFs). Our results show that plasminogen activator inhibitor type 1 and type 2 (PAI-1 and PAI-2) expression is significantly increased in Cav-1$^{-/-}$ MSFs. To establish a direct cause-effect relationship, we next generated immortalized human fibroblast lines stably overexpressing either PAI-1 or PAI-2. Importantly, PAI-1/2(+) fibroblasts promote the growth of MDA-MB-231 tumors (a human breast cancer cell line) in a murine xenograft model, without any increases in angiogenesis. Similarly, PAI-1/2(+) fibroblasts stimulate experimental metastasis of MDA-MB-231 cells using an in vivo lung colonization assay. Further mechanistic studies revealed that fibroblasts overexpressing PAI-1 or PAI-2 display increased autophagy ("self-eating") and are sufficient to induce mitochondrial biogenesis/activity in adjacent cancer cells, in co-culture experiments. In xenografts, PAI-1/2(+) fibroblasts significantly reduce the apoptosis of MDA-MB-231 tumor cells. The current study provides further support for the "Autophagic Tumor Stroma Model of Cancer" and identifies a novel "extracellular matrix"-based signaling mechanism, by which a loss of stromal Cav-1 generates a metastatic phenotype. Thus, the secretion and remodeling of extracellular matrix components (such as PAI-1/2) can directly regulate both (1) autophagy in stromal fibroblasts and (2) epithelial tumor cell mitochondrial metabolism.

Introduction

Tumors are heterogeneous, and their growth depends on reciprocal interactions between genetically altered epithelial cells and their surrounding stromal microenvironment.[1,2] The tumor microenvironment contains a variety of cell types, including endothelial and immune cells, pericytes, mesenchymal stem cells and fibroblasts. As a tumor develops, normal fibroblasts undergo reprogramming, through their reciprocal interactions with cancer cells, acquiring a more myofibroblastic phenotype.[3,4] Such activated fibroblasts are commonly known as cancer-associated fibroblasts (CAFs) and promote the progression, uncontrolled growth and metastatic spread of cancers, although the exact mechanism(s) underlying these effects are poorly understood.[4-7]

Mounting evidence indicates that downregulation of Cav-1 leads to an activated phenotype in fibroblasts. Thus, it has been suggested that loss of Cav-1 in fibroblasts is a biomarker of CAFs.[8-10] In particular, we showed that mammary stromal fibroblasts (MSFs) derived from Cav-1-knockout (KO) mice exhibit many human CAF-like characteristics. Importantly, gene profiles derived from Cav-1 KO MSFs are associated with poor clinical outcome in breast cancer patients treated with tamoxifen monotherapy.[9] In support of these findings, mammary fat pads of Cav-1 KO mice stimulate the growth (up to ~2-fold) of implanted

*Correspondence to: Remedios Castello-Cros and Michael P. Lisanti; Email: remedios.castello@jefferson.edu and michael.lisanti@kimmelcancercenter.org
Submitted: 04/18/11; Accepted: 04/25/11
DOI: 10.4161/cc.10.12.16002

mammary tumor tissue, indicating that the mammary tumor stroma of Cav-1 KO mice has tumor-promoting properties.[11] In addition, we have recently shown that human fibroblasts lacking Cav-1 significantly promote the tumor growth of MDA-MB-231 cells (~4-fold) in co-injection experiments.[12]

We and others have identified an absence of stromal caveolin-1 (Cav-1) as a new biomarker for predicting clinical outcome in human breast cancer patients.[13-17] The loss of Cav-1 in the cancer-associated fibroblast compartment correlates with early tumor recurrence, lymph node metastasis and tamoxifen-resistance. Absence of stromal Cav-1 is a predictive biomarker independent of clinicopathologic features or breast cancer subtype (ER^+, PR^+, $HER2^+$ and triple-negative tumors).[16] Also, lack of stromal Cav-1 expression in dutal carcinoma in situ (DCIS) lesions is predictive of progression to invasive breast cancer.[14] We have also shown that an absence of stromal Cav-1 is a biomarker for tumor progression to metastatic disease (to lymph-nodes and bone) in human prostate cancer.[18] Therefore, a stroma lacking Cav-1 may promote the aggressiveness of a variety of different human cancer types.[13]

Based on these findings, we recently proposed a new hypothesis for understanding how tumors evolve, called the "autophagic tumor stroma model of cancer cell metabolism."[19,20] In this model, cancer cells induce the downregulation of Cav-1 in the adjacent fibroblasts via oxidative stress. Consequently, the loss of Cav-1 induces the autophagic destruction of mitochondria (mitophagy) in CAFs, which drives the fibroblastic production of recycled high-energy metabolites.[21] These energy-rich metabolites are then taken up by the adjacent cancer cells to promote mitochondrial biogenesis and "feed" their anabolic metabolism, thereby driving their growth and protecting these cancer cells against apoptosis.[22,23] Thus, loss of stromal Cav-1 leads to a "nutrient-rich" tumor microenvironment, which promotes the invasive growth and metastatic dissemination of cancer cells. However, the downstream mediator(s) of the tumor-promoting effects of a loss of Cav-1 in CAFs are not yet known.

The urokinase-type plasminogen activator (uPA) system plays an important and multifaceted role in cancer pathogenesis.[24] uPA, when bound to its receptor (uPA-R), actively converts plasminogen into the mature broad spectrum serine protease, plasmin, which in turn degrades extracellular matrix (ECM) proteins and activates latent growth factors and matrix metalloproteases (MMPs), facilitating invasion and metastatic spread of cancer cells.[24] The activity of uPA is regulated by the plasminogen activator inhibitors type-1 and -2 (PAI-1 and PAI-2), which belong to the serpin (serine protease inhibitor) superfamily, and are also known as SERPINE1 and SERPINB2, respectively.[25]

Paradoxically, high levels of PAI-1 and PAI-2 correlate with a poor and good prognosis, in breast cancer and other types of cancers, respectively.[26-31] Notably, PAI-1 and uPA were among the first tumor markers to be validated at the highest level of evidence (LOE I) regarding their clinical utility for breast cancer.[32] In most of these studies, PAI-1 and PAI-2 levels have been determined by ELISA in whole-tumor tissue extracts without dissecting whether their prognostic value lies in the tumor stroma or the tumor epithelial cells. Umeda et al., using in situ hybridization analysis, showed that, whereas PAI-1 and PAI-2 mRNA's were not detected in fibroblasts of normal breast or DCIS, these inhibitors were highly expressed in fibroblasts of invasive breast cancers.[33] In addition, the protein expression of PAI-1 and PAI-2 was elevated in the fibroblastic compartment of breast cancer tissues.[34-36] However, the relevance of fibroblasts expressing high levels of PAI-1 or PAI-2 in breast cancer malignancy remains poorly defined.

Here, we investigated the signaling mechanism(s) by which a loss of stromal Cav-1 in the fibroblast compartment contributes to PAI-1 and PAI-2 activity, leading to enhanced breast pathology. To that end, we performed a comparative proteomic analysis of murine wild-type and Cav-$1^{-/-}$ knockout mammary fibroblasts. Our results show that loss of Cav-1 in mammary fibroblasts leads to upregulation of PAI-1 and PAI-2 protein expression. Fibroblasts overexpressing PAI-1 or PAI-2, were able to promote breast tumor growth and metastasis. Mechanistically, these fibroblasts, which exhibit elevated expression of autophagic markers, stimulate anabolic metabolism and prevent the apoptotic cell death of adjacent cancer cells. As such, the tumor promoting properties of fibroblasts overexpressing PAI-1 or PAI-2 may be explained by our novel view of tumor metabolism, the "autophagic tumor stroma model of cancer cell metabolism."

Therefore, the current study provides direct evidence that PAI-1 and PAI-2 are implicated in the breast tumor-promoting effects of Cav-1-deficient fibroblasts.

Results

Loss of Cav-1 in mammary stromal fibroblasts upregulates plasminogen activator type 1 and type 2 (PAI-1 and PAI-2). In order to generate new insight into the mechanism(s) by which a loss of stromal Cav-1 participates in mammary tumorigenesis, we performed an unbiased comparative proteomic analysis of cell lysates and conditioned media from wild-type (WT) and Cav-1-knockout (KO) mammary stromal fibroblasts (MSFs).

As shown in **Tables 1 and 2**, a number of proteins upregulated in Cav-1 KO MSFs are those seen in associated with activated fibroblasts (VIM, FN1, COL1A1 and P4HB). This is in agreement with our previous studies, showing that a loss of Cav-1 in fibroblasts induces a myofibroblastic phenotype.[9,12,19,37] Also, the expression of the two principal inhibitors of uPA, namely PAI-1 (SERPINE1) and PAI-2 (SERPINB2), was upregulated in Cav-1 KO MSFs. Increased expression of PAI-1 was validated by western blotting and immunofluorescence analysis of Cav-1 KO MSFs and their derived extracellular matrices (**Fig. 1A–C**). The differential expression of PAI-2 was also validated by western blotting (**Fig. 1D**). Similarly, the stroma of invasive human breast tumors (pre-screened for a lack stromal Cav-1) displays strong expression of PAI-1 and PAI-2 in the fibroblast compartment (**Fig. 2**). Therefore, loss of Cav-1 in mammary stromal fibroblasts leads to upregulation of PAI-1 and PAI-2 expression in cultured fibroblasts in vitro and in human tumors in vivo.

Overexpression of PAI-1 or PAI-2 in fibroblasts induces myofibroblastic features. We have previously show that downregulation of Cav-1 in fibroblasts leads to the acquisition of a

Table 1. Proteomic analysis of upregulated proteins in cell lysates from Cav-1$^{-/-}$ null MSFs

	Fold change KO/WT	Accession number	Spot number
Protein folding			
Heat shock 70 kDa protein 1A (HSPA1A)	2.37	gi|32451998	19
Chaperonin containing Tcp1, subunit 6A (zeta1) (CCT6A)	2.19	gi|6753324	24
Extracellular matrix homeostasis			
Serpin peptidase inhibitor, clade B (ovalbumin), member 2 (SERPINB2) (a.k.a., PAI-2)	2.6	gi|6755098	39
Cytoskeleton			
Vimentin (VIM)	2.17	gi|2078001	33
Cell cycle			
Ptms protein (PTMS)	2.76	gi|51593432	64
Others			
transmembrane protein with EGF-like and 2 follistatin-like domains 1 (TMEFF1)	2.89	gi|148670383	57
Hemoglobin, α1 (HBA1)	2.87	gi|553919	54
Signal sequence receptor, β (translocon-associated protein β) (SSR2)	2.31	gi|148683319	65
Unnamed protein product	3.2	gi|12842671	15

All peptide sequences used for protein identification correspond to the *Mus musculus* protein product, ruling out contamination by serum proteins. WT, wild-type mammary stromal fibroblasts; KO, Cav-1-knockout mammary stromal fibroblasts.

Table 2. Proteomic analysis of proteins in the conditioned media from Cav-1$^{-/-}$ MSFs

	Fold change KO/WT	Accession number	Spot number
Extracellular matrix proteins			
Fibronectin 1 (FN1)	3.55	gi|219518597	5
Periostin, osteoblast specific factor (POSTN)	3.17	gi|148703313	19
Collagen, type I, α1 (COL1A1)	2.24	gi|34328108	4a
Collagen, type III, α1 (COL3A1)	2.07	gi|20380522	56
Extracellular matrix homeostasis			
Serpin peptidase inhibitor, clade E (nexin, plasminogen activator inhibitor type 1), member 1 (SERPINE1) (a.k.a., PAI-1)	2.84	gi|170172562	43
Prolyl 4-hydroxylase, β polypeptide (P4HB)	1.91	gi|148702818	35
Other			
Chaperonin containing Tcp1, subunit 6a (zeta) (CCT6A)	2.71	gi|62948125	38
Non-metastatic cells 2, protein (NM23B) expressed in (NME2)	2.25	gi|6679078	64
Non-metastatic cells 2, protein (NM23B) expressed in (NME2)	1.52	gi|6679078	66

All peptide sequences used for protein identification correspond to the *Mus musculus* protein product, ruling out contamination by serum proteins. WT, wild-type mammary stromal fibroblasts; KO, Cav-1-knockout mammary stromal fibroblasts.

myofibroblastic phenotype.[9,12,37] Furthermore, both PAI-1 and PAI-2 have been found to be upregulated in human cancer-associated fibroblasts (CAFs) as compared with normal fibroblasts.[34,35] Thus, we decided to investigate whether overexpression of PAI-1 or PAI-2 in fibroblasts induces myofibroblastic characteristics. To address this issue, we first stably overexpressed PAI-1 or PAI-2 in immortalized human hTERT-BJ1 fibroblasts (**Fig. 3A and B**). Overexpression of PAI-1 or PAI-2 did not alter Cav-1 levels in these fibroblasts when compared with controls (empty vector-transduced hTERT-BJ1 fibroblasts). In addition, these two proteins were not reciprocally regulated when overexpressed (**Fig. 3C**).

Next, we examined myofibroblastic traits in these fibroblasts. We found that overexpression of PAI-1 or PAI-2 upregulated calponin and vimentin, two known myofibroblastic markers (**Fig. 4A–C**). Moreover, PAI-1, but not PAI-2, fibroblasts exhibited elevated expression (**Fig. 4C**) and deposition (**Fig. 4D**) of fibronectin, which is characteristic of activated fibroblasts. Taken together, our results suggest that PAI-1 and PAI-2 are downstream targets of Cav-1, and they may contribute to the acquisition of a myofibroblastic phenotype of Cav-1-deficient fibroblasts.

Fibroblasts overexpressing PAI-1 or PAI-2 promote breast tumor growth, without affecting angiogenesis. Next, we evaluated whether fibroblasts overexpressing PAI-1 or PAI-2 can

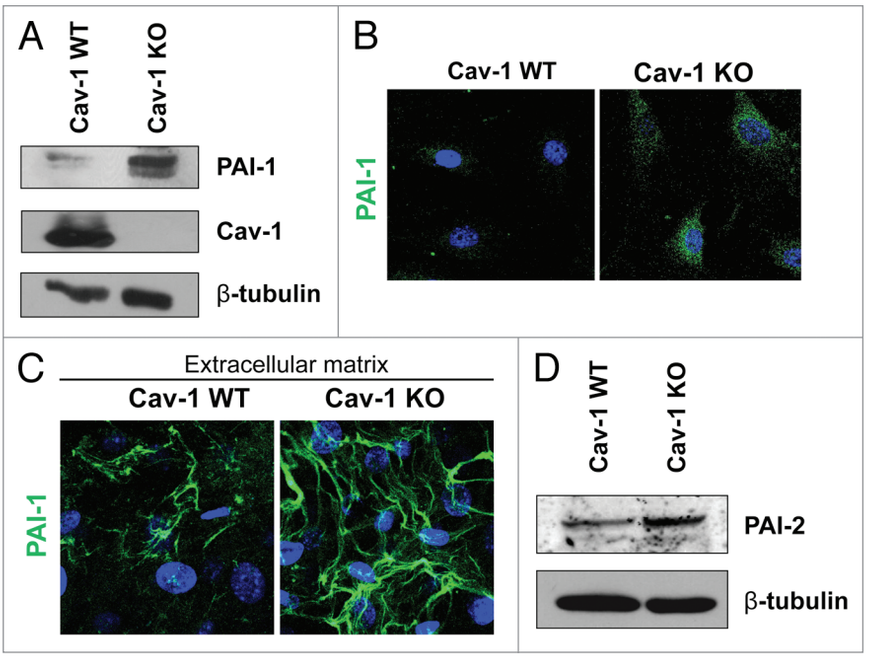

Figure 1. Validation of the proteomic data for PAI-1 and PAI-2. To confirm the relative changes in PAI-1 and PAI-2 protein expression observed in the proteomic analysis, wild-type and Cav-1 KO MSFs were subjected to immunoblot and immunofluorescence analyses with antibodies directed against PAI-1 and PAI-2. (A) Western blotting for PAI-1. Note that PAI-1 expression is upregulated in Cav-1 KO MSFs. Immunoblotting with β-tubulin is shown as a control for equal loading. (B) Intracellular localization of PAI-1. Note that PAI-1 expression is increased in Cav-1 KO MSFs. Nuclei were immunostained with Hoechst (blue). Images captured at original magnification of 63x. (C) Localization of PAI-1 in fibroblast-derived extracellular matrices. Wild-type and Cav-1 KO MSFs were plated onto gelatin cross-linked coverslips. Fresh medium containing ascorbic acid was added every other day for 5 d to induce production of extracellular matrix. Unextracted matrices were then fixed and immunostained with antibodies against PAI-1. Note that PAI-1 is elevated in Cav-1 KO MSF-derived extracellular matrices, indicating an increased secretion of PAI-1 by Cav-1 KO MSFs. Nuclei were immunostained with Hoechst (blue). Images were captured at original magnification 63x. (D) Immunoblotting for PAI-2. Note that PAI-2 expression is upregulated in Cav-1 KO MSFs. Immunoblotting with β-tubulin is shown as a control for equal loading.

phenocopy the tumor-promoting effects of fibroblasts lacking Cav-1.[12] For this purpose, we co-cultured fibroblasts and human breast cancer cells [MDA-MB-231 (GFP$^+$)] and determined the GFP intensity for several days. **Figure 5** shows that fibroblasts overexpressing PAI-1 or PAI-2 promoted the growth of MDA cells in vitro. In order to assess whether these fibroblasts were able to promote tumor growth in vivo, we co-injected a mixture of MDA-MB-231 cells and fibroblasts in the flanks of nude mice. After 3 weeks, the tumors were removed and their weights and volumes were determined. Fibroblasts overexpressing PAI-1 or PAI-2 significantly increased tumor mass, ~3-to-4-fold (**Fig. 6A**), and tumor volume, ~4-fold (**Fig. 6B**). Interestingly, no significant differences in blood vessel density (number of vessels per mm^2) were observed among the three groups (**Fig.** 7). In accordance with the in vitro studies (**Fig. 4C and D**), we found that tumors grown in the presence of PAI-1-overexpressing fibroblasts exhibited increased stromal deposition of fibronectin (**Fig.** 7C).

Collectively, these results indicate that fibroblasts overexpressing PAI-1 or PAI-2 stimulate mammary tumor growth independently of angiogenesis.

Fibroblasts overexpressing PAI-1 or PAI-2 display elevated autophagy and promote the anabolic metabolism of adjacent tumor cells. Since an increase in tumor angiogenesis could not explain the tumor-promoting properties of PAI-1 and PAI-2 fibroblasts, we examined whether the increased tumor growth could be explained by metabolic interactions between fibroblasts and tumor cells.[19,23]

To test this hypothesis, we first evaluated the levels of autophagic markers in fibroblasts overexpressing PAI-1 or PAI-2. Autophagy is characterized by the formation of acidic vesicular organelles (AVOs), which can be detected using acridine orange. This reagent is a weak base that, when unprotonated, appears as green fluorescence. However, when it penetrates into an acidic compartment, it is protonated and forms aggregates and appears bright red.[38,39] Vital staining of fibroblasts with acridine orange revealed that fibroblasts overexpressing PAI-1 or PAI-2 displayed a larger amount of AVOs than control fibroblasts (**Fig. 8A**). Also, overexpression of PAI-1 or PAI-2 upregulated the expression of the autophagic markers, Beclin-1, LAMP-1 and LAMP-2 (**Fig. 8B and C**). Given that autophagy negatively regulates the cell cycle, we assessed the effects of PAI-1 or PAI-2 overexpression on fibroblast proliferation by measuring BrdU incorporation. We observed a decrease in proliferation of fibroblasts overexpressing PAI-1 and PAI-2 as compared with the vector alone control (**Fig. 8D**). These results suggest that overexpression of PAI-1 or PAI-2 induces autophagy in fibroblasts.

To assess whether fibroblasts with increased expression of PAI-1 or PAI-2 were able to promote the anabolic metabolism of tumor cells, we immunostained co-cultures of fibroblasts and breast cancer cells [MDA-MB-231 GFP(+)] with an antibody directed against the intact mitochondrial membrane (MAB1273). **Figure 9** shows that fibroblasts overexpressing PAI-1 or PAI-2 strikingly increased the mitochondria mass of MDA-MD-231 cells as compared with control fibroblasts. Interestingly, low mitochondrial mass was observed in fibroblasts in these co-cultures (**Fig. 9**). Taken together, these data suggest that fibroblasts overexpressing PAI-1 or PAI-2 promote increased oxidative mitochondrial metabolism in adjacent cancer cells.

Fibroblasts overexpressing PAI-1 or PAI-2 promote tumor cell survival. We have previously reported that the metabolic-coupling between cancer cells and fibroblasts results in a reduction of epithelial cancer cell apoptosis.[22] Therefore, we assessed apoptosis using a tunnel assay in tumors resulting from the co-injection of fibroblasts with MDA-MB-231 cells. As shown in **Figure 10**, fibroblasts overexpressing PAI-1 or PAI-2 significantly

decreased the apoptosis of MDA-MB-231 cells in vivo. Reductions in tumor cell apoptosis were more pronounced with fibroblasts overexpressing PAI-2, than with those overexpressing PAI-1 (**Fig. 10**). However, no statistically significant differences were observed in tumor cell proliferation (**Fig. 11A**). The ratio of mitotic vs. apoptotic tumor cells was significantly increased in tumors containing fibroblasts overexpressing PAI-1 or PAI-2 as compared with tumors grown in the presence of control fibroblasts (**Fig. 11B**). These data indicate that fibroblasts overexpressing PAI-1 or PAI-2 protect breast cancer cells against apoptotic cell death. Thus, these results support our previous observations that autophagic fibroblasts, in addition to providing nutrients, prevent the death of adjacent cancer cells.[22]

Fibroblasts overexpressing PAI-1 or PAI-2 increase the metastatic spread of breast cancer cells. In order to determine whether fibroblasts overexpressing PAI-1 or PAI-2 affect the metastatic capacity of breast cancer cells, we co-injected fibroblasts with MDA-MB-231 (GFP$^+$) cells into the tail vein of nude mice. After 7 weeks, the lungs were surgically excised and examined for lung metastases.

As shown in **Figure 12**, fibroblasts overexpressing PAI-1 or PAI-2 significantly increase the ability of MDA-MB-231 (GFP$^+$) to form lung metastases by ~4-to-5-fold. Taken together, these data suggest that fibroblasts overexpressing PAI-1 or PAI-2 promote the metastatic potential of breast cancer cells.

Discussion

Here, we investigated the signaling mechanism(s) implicated in the breast tumor-promoting microenvironment induced by the loss of stromal Cav-1. Unbiased proteomic analysis of Cav-1 wild-type and knockout mammary gland fibroblasts revealed that a loss of Cav-1 in mammary fibroblasts leads to the upregulation of both PAI-1 and PAI-2. Fibroblasts overexpressing PAI-1 or PAI-2 were able to significantly increase both tumor growth and metastasis of human breast cancer cells. Thus, the current study provides additional novel biomarkers of CAFs and, potentially, new therapeutic targets for stromal-based treatment interventions.

We have previously demonstrated that a loss of stromal Cav-1 in cancer-associated fibroblasts[8] is a powerful and single independent predictor of clinical outcome in human breast cancers.[13-16] To understand the strong prognostic value of mammary fibroblasts lacking Cav-1, we turned to Cav-1-knockout (KO) mammary stromal fibroblasts (MSFs), as a model for Cav-1 deficient cancer-associated fibroblasts.[9] Proteomic analysis revealed that loss of Cav-1 in mammary fibroblasts leads to an increase of plasminogen activator inhibitor type-1 and type-2 (PAI-1 and PAI-2). However, overexpression of PAI-1 or PAI-2 in human fibroblasts did not affect Cav-1

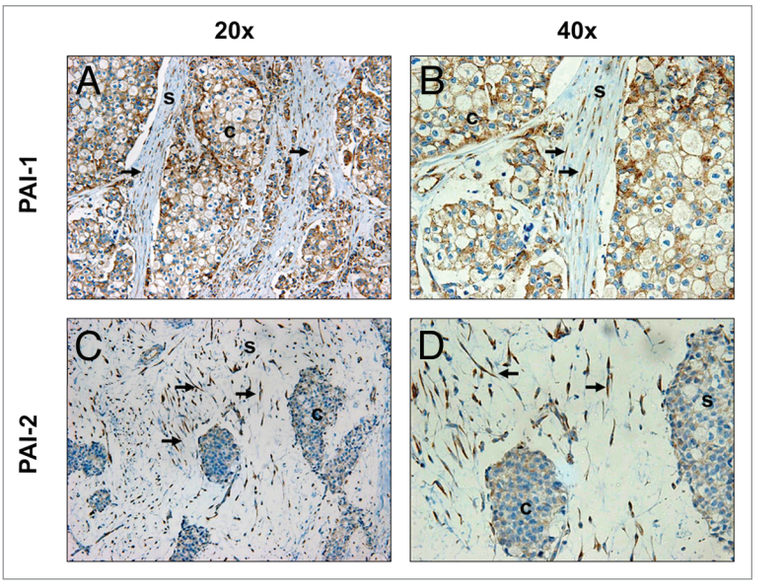

Figure 2. Expression of PAI-1 and PAI-2 is elevated in Cav-1-deficient fibroblasts of human breast cancer tissues. Paraffin-embedded sections of human breast cancer tissues lacking stromal Cav-1 were immunostained with antibodies directed against PAI-1 (A and B) and PAI-2 (C and D). Slides were counterstained with hematoxylin. Note that PAI-1 stained positive in both stromal and cancer cells, whereas PAI-2 expression is observed only in stromal cells. White arrows indicate Cav-1-deficient fibroblasts that stained positive for both PAI-1 and PAI-2. Images were captured at an original magnification of 20x and 40x. s, stromal cells; c, cancer cells.

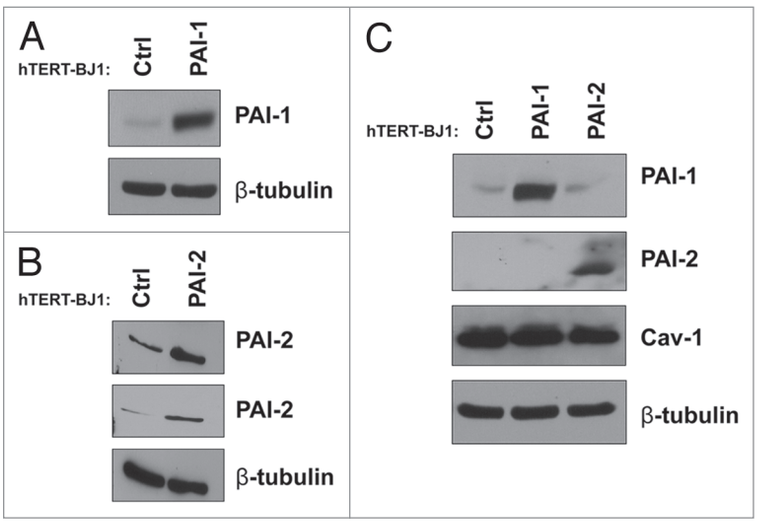

Figure 3. Recombinant overexpression of PAI-1 or PAI-2 does not alter Cav-1 expression levels. To assess the regulation of Cav-1 by PAI-1 and PAI-2 in fibroblasts, we stably overexpressed PAI-1 or PAI-2 in immortalized human fibroblasts (hTERT-BJ1) using lentiviral vectors. As a control (Ctrl), hTERT-BJ1 fibroblasts were transduced with an empty vector. The overexpression of PAI-1 and PAI-2 was confirmed by western blot (A and B), respectively. Immunoblotting with β-tubulin is shown as a control for equal loading. (C) The expression of Cav-1 in fibroblasts overexpressing PAI-1 or PAI-2 was assessed by western blotting. Note that no differences in Cav-1 levels were observed. Immunoblottings for PAI-1 and PAI-2 are also displayed. Immunoblotting for β-tubulin is shown as a control for equal loading.

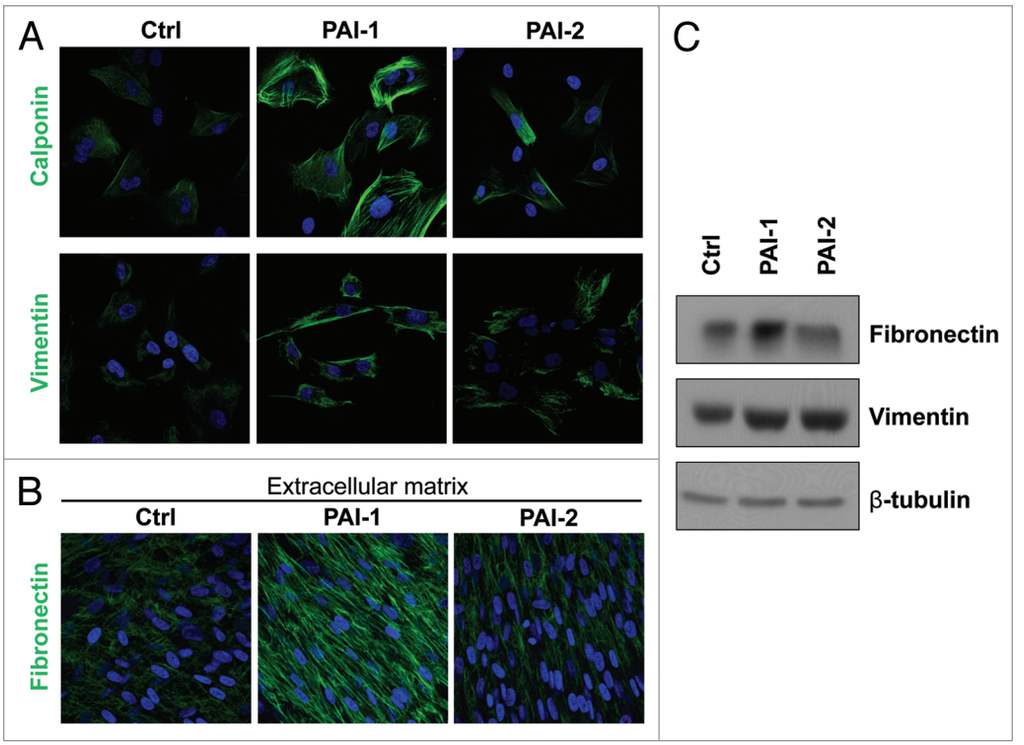

Figure 4. Overexpression of PAI-1 or PAI-2 leads to the upregulation of myofibroblastic markers. To evaluate whether the overexpression of PAI-1 and PAI-2 phenocopy the myofibroblastic phenotype of Cav-1-deficient fibroblasts, the expression of several myofibroblastic markers was assessed in fibroblast control or overexpressing PAI-1 or PAI-2. (A) Localization of calponin (upper parts) and vimentin (lower parts). Note that overexpression of PAI-1 or PAI-2 upregulates the levels of two myofibroblastic markers, calponin and vimentin. Nuclei were immunostained with Hoechst (blue). Images captured at original magnification of 63x. (B) Immunoblotting for vimentin and fibronectin. Note that overexpression of PAI-1 or PAI-2 upregulates vimentin and the overexpression of PAI-1 increases the expression of fibronectin. Immunoblotting with β-tubulin is shown as a control for equal loading. (C) Localization of fibronectin in fibroblast-derived extracellular matrices. Fibroblasts overexpressing PAI-1 or PAI-2 along with controls were plated onto gelatin cross-linked coverslips. Fresh medium containing ascorbic acid was added every other day for 5 d to induce extracellular matrix production. Then, the cells with their matrices were fixed and immunostained with an antibody against fibronectin. Note that PAI-1 overexpression increases fibronectin deposition, a myofibroblastic marker. Nuclei were counterstained with Hoechst (blue). Images captured at original magnification of 63x. Ctrl, fibroblasts containing empty vector alone; PAI-1, fibroblasts overexpressing PAI-1; PAI-2, fibroblasts overexpressing PAI-2.

levels, suggesting that PAI-1 and PAI-2 are downstream targets of Cav-1. Consistent with our findings, Lee et al. showed that the overexpression of Cav-1 downregulates PAI-1 in NIH-3T3 fibroblasts.[40] Also, we previously demonstrated that Cav-1$^{-/-}$ immortalized mouse embryonic fibroblasts (MEFs) exhibit a near 10-fold increase in PAI-2 as compared with those expressing Cav-1.[41,42]

PAI-1 and PAI-2 are the principal inhibitors of urokinase-type plasminogen activator (uPA), which is implicated at multiple stages of tumor formation and progression, such as ECM degradation, cell migration, adhesion and proliferation.[24] High levels of PAI-1 are caused by a number of mechanisms, including by activated HIF1-α[42] and NFκB,[43] and PAI-2 expression is increased by a variety of inflammatory stimuli.[44] We have previously observed that loss of Cav-1 in stromal cells results in ROS overproduction, which in turn activate HIF1-α and NFκB, the latter leading to the upregulation of inflammatory mediators.[45,46] Therefore, we speculate that the increased expression of PAI-1 and PAI-2 observed in Cav-1-deficient fibroblasts may be a consequence of the oxidative stress produced by the loss of Cav-1.

In agreement with our previous studies,[9,12,19,37] here we observe that loss of Cav-1 in fibroblasts results in the upregulation of CAF markers, such as vimentin, PH4B, fibronectin and collagen. Therefore, these data support the notion that a loss of Cav-1 drives the onset of a myofibroblastic phenotype. We also show that overexpression of PAI-1 or PAI-2 leads to increased expression of myofibroblastic markers in human fibroblasts, suggesting that these uPA inhibitors may contribute to the acquisition of a CAF-like phenotype, induced by the loss of Cav-1.

We set out to determine whether we could phenocopy the tumor promoting effects of a loss of Cav-1 in fibroblasts, using these newly discovered down-stream targets, namely PAI-1 and PAI-2. Recently, using a mouse xenograft model, we have shown that downregulation of Cav-1 in human fibroblasts results in ~4-fold increase in MDA-MB-231 tumor growth.[12] Using the same xenograft model, here we observe, for the first time, that fibroblasts overexpressing PAI-1 or PAI-2 significantly increase tumor mass (~3-to-4-fold) and tumor volume (~4-fold). In addition, these fibroblasts when co-injected with MDA-MB-231 cells increased their metastatic potential. Mechanistically, we show that PAI-1- and PAI-2-expressing fibroblasts exhibit increased

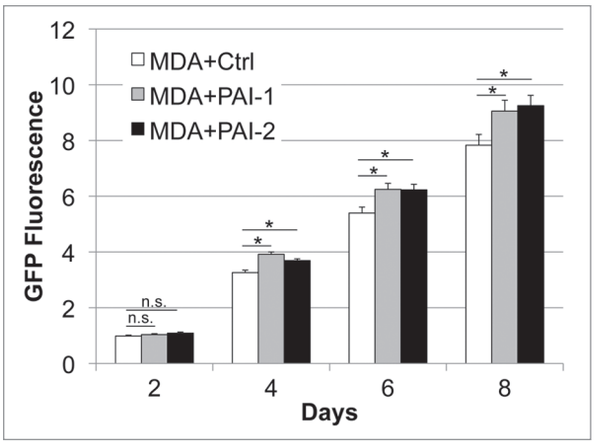

Figure 5. Fibroblasts overexpressing PAI-1 or PAI-2 promote tumor growth in vitro. Fibroblasts (control vs. those overexpressing PAI-1 or PAI-2) were co-cultured with MDA-MB-231 GFP$^+$ (MDA) cells in a 5:1 ratio. The fluorescence was determined (as a measurement of MDA growth) every other day for 8 d and normalized to the fluorescence intensity of the first day to avoid differences due to cell attachment. Note a significant increase in MDA growth in the presence of fibroblasts overexpressing PAI-1 or PAI-2 compared with controls, after the fourth day of co-culture. Results are represented as mean ± SEM. n.s., not significant. An asterisk indicates that $p \leq 0.05$. Ctrl, fibroblasts containing empty vector alone; PAI-1, fibroblasts overexpressing PAI-1; PAI-2, fibroblasts overexpressing PAI-2; MDA, MDA-MB-231 (GFP$^+$).

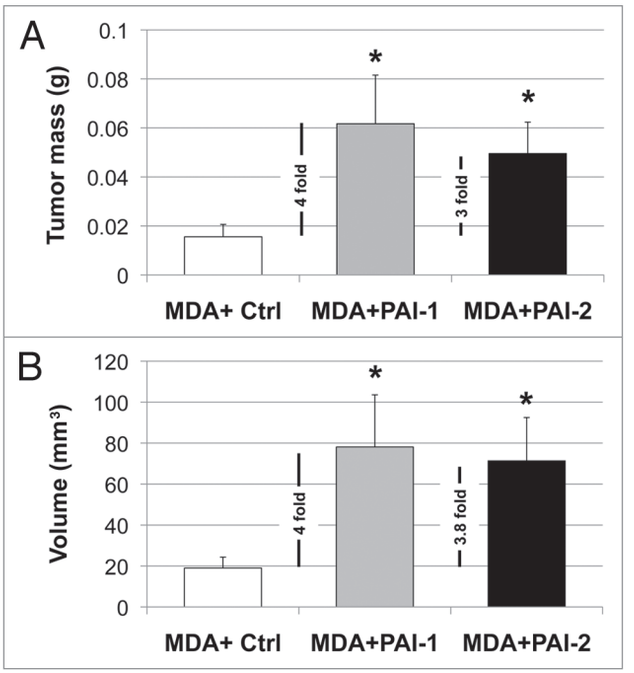

Figure 6. Fibroblasts overexpressing PAI-1 or PAI-2 promote tumor growth in vivo. To determine whether overexpression of PAI-1 or PAI-2 can phenocopy the tumor-promoting effects of Cav-1-deficient fibroblasts, fibroblasts (control vs. those overexpressing PAI-1 or PAI-2) were co-injected with a human breast cancer cell line [MDA-MB-231 (GFP$^+$) cells] (MDA) in the flanks of nude mice. After 3 weeks, the tumors that formed were harvested and subjected to a detailed analysis. Note that relative to controls, PAI-1 or PAI-2 expressing fibroblasts increased tumor mass by ~3-to-4-fold (A) and tumor volume by ~4-fold. (B) Results are represented as the mean ± SEM. An asterisk indicates that $p \leq 0.05$ compared with controls. n = 10 flank injections for each experimental group. Ctrl, fibroblasts containing empty vector alone; PAI-1, fibroblasts overexpressing PAI-1; PAI-2, fibroblasts overexpressing PAI-2; MDA, MDA-MB-231 (GFP$^+$).

expression of autophagic markers and, in co-cultures, these fibroblasts increase mitochondrial biomass in adjacent cancer cells. These data directly support our novel hypothesis explaining tumor development, which we have termed the "autophagic tumor stroma model of cancer cell metabolism."[19,20] According to this hypothesis, cancer cells use oxidative stress as a weapon to induce autophagy in adjacent fibroblasts. Consequently, autophagic fibroblasts provide energy-rich nutrients that are taken up by adjacent cancer cells to "fuel" oxidative mitochondrial metabolism and promote tumor growth.[21-23] In support of this notion, we demonstrated previously that systemic administration of energy-rich metabolites, such as the ketones and L-lactate, is sufficient to promote both tumor growth and metastasis, using MDA-MB-231 cells.[47]

The current study reveals that PAI-1- or PAI-2-expressing fibroblasts promote breast tumor growth without altering angiogenesis. Similarly, fibroblasts harboring HIF1α or NFκB, also exhibit increased expression of autophagic markers and promote the tumor growth of MDA-MB-231 cells without affecting blood vessel density.[21] Therefore, the current study supports our previous hypothesis that autophagic fibroblasts have the ability to promote tumor growth independent of angiogenesis. This may explain the failure of many angiogenic inhibitors in providing clinical benefits in recent therapeutic cancer trials.

The finding that PAI-1 is able to induce autophagy in fibroblasts may explain previous paradoxical results about the role of PAI-1 in cancer pathogenesis. More specifically, it may explain why high levels of PAI-1 predict poor prognosis in a variety of cancer types,[26,27,29] but its expression in cancer cells by transfection reduces the invasiveness and metastasis of tumor cells.[48,49] It is likely that PAI-1 expression in cancer cells leads to autophagy and, consequently, reduces their aggressiveness; however, the autophagy induced by PAI-1 in the host fibroblasts may provide energy-rich metabolites that promote tumor growth. In agreement with this hypothesis, we recently demonstrated that the expression of active HIF1α, one of the transcription factors known to upregulate PAI-1, promotes tumor growth when it is expressed in fibroblasts; conversely, activated HIF1α in cancer cells dramatically suppressed tumor growth.[21] In addition, strong expression of PAI-1 in the fibroblast compartment, rather than in cancer cells, has the greatest impact on the clinical behavior of breast cancer.[36] Therefore, these data suggest that the source of PAI-1 (its compartment-specific origin) is an important determinant of prognosis.

We also observe that PAI-1 and PAI-2-overexpressing fibroblasts significantly reduce the apoptosis of MDA-MB-231, without alterations in proliferation. In agreement with these results, we have previously found, using MCF7 co-cultures, that Cav-1-deficient fibroblasts protect adjacent breast cancer cells against apoptosis.[22] This supports the notion that autophagic fibroblasts, in addition to providing nutrients to "fuel" anabolic metabolism,

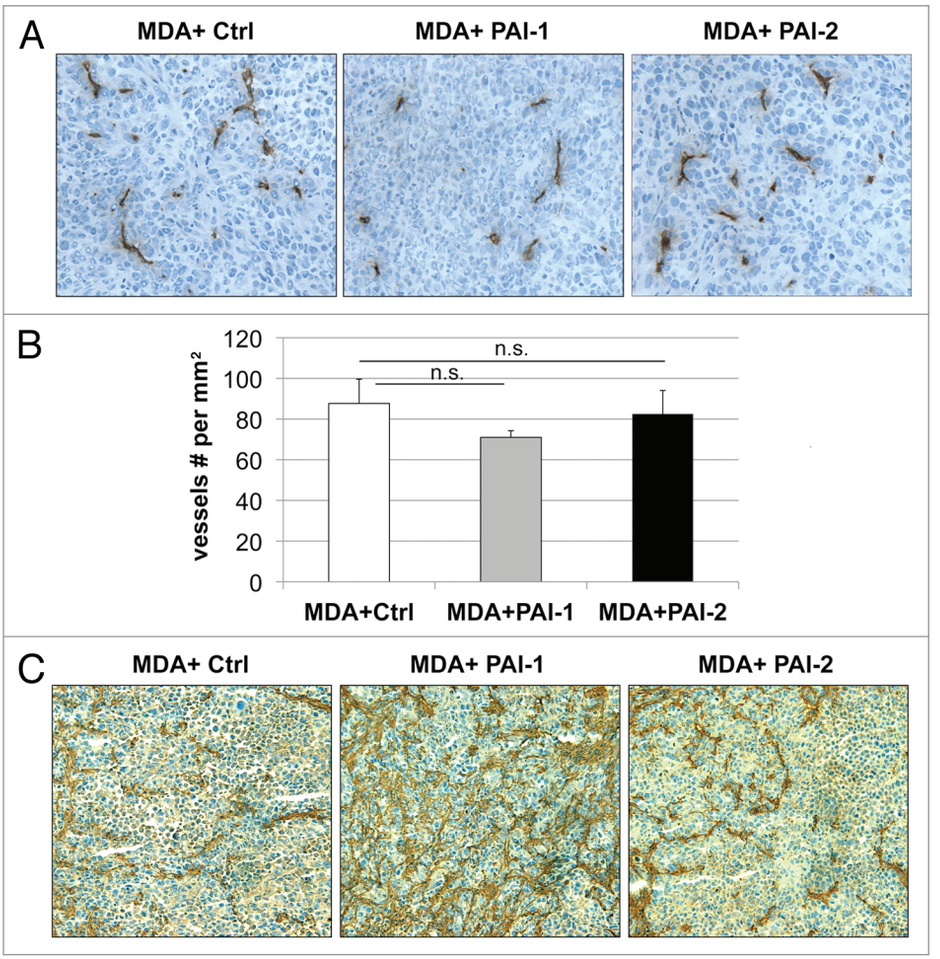

Figure 7. Fibroblasts overexpressing PAI-1 or PAI-2 do not affect tumor angiogenesis. Paraffin-embedded tumor sections from MDA-MB-231 cells (grown the presence of control fibroblasts or fibroblasts overexpressing PAI-1 or PAI-2) were immunostained with anti-CD31 antibodies and vessel density was determined. (A) Representative images for CD-31 immuno-staining are shown. Slides were counterstained with hematoxylin. Images were captured at 20x. (B) Quantification of the CD-31-positive vessels. Note that no significant differences in vessel density were observed. Results are represented as the mean ± SEM; n.s., not significant. (C) Immunhistochemical analysis of fibronectin. Note that MDA-MB-231 cells grown in the presence of fibroblasts overexpressing PAI-1 exhibit increased deposition of fibronectin in the stromal compartment. Images were captured at 20x. Ctrl, fibroblasts containing empty vector alone; PAI-1, fibroblasts overexpressing PAI-1; PAI-2, fibroblasts overexpressing PAI-2; MDA, MDA-MB-231 (GFP^+).

also play a protective role in preventing cell death in adjacent cancer cells. Significantly, TGFβ-treated prostate stromal cells underwent myofibroblastic differentiation and decreased the apoptotic rate of co-cultured prostate cancer cells.[50] We have previously shown that Cav-1 knockdown in fibroblasts is sufficient to activate the TGFβ signaling pathway,[37,51] which is known to regulate PAI-1 expression.[52] Therefore, we speculate that a loss of Cav-1 in fibroblasts may lead to TGFβ activation that, in turn, increases PAI-1 expression, protecting cancer cells against apoptosis.

In conclusion, we show that a loss of Cav-1 in mammary fibroblasts results in an increase of PAI-1 and PAI-2. Importantly, fibroblasts overexpressing PAI-1 or PAI-2 phenocopy the tumor-promoting effects of Cav-1-deficient fibroblasts. Consequently, targeting PAI-1 and PAI-2 in fibroblasts may be a novel therapeutic strategy to inhibit the activated tumor microenvironment induced by a loss of stromal Cav-1.

Materials and Methods

Materials. Antibodies were obtained from commercial sources: anti-PAI-1 (for WB and IF: sc-8979, Santa Cruz Biotech, for IHC: HPA020559, Sigma), anti-PAI-2 (for WB: sc-7646 Santa Cruz Biotech for mouse cells and #3750 from American diagnostic for human cells, for IHC: HPA015480, from Sigma), anti-β-tubulin (for WB: #T4026, Sigma), anti-caveolin-1 (for WB: sc-894, N20, Santa Cruz Biotech), anti-vimentin (for IF: M0725, Dako; for WB: #3932, R28; Cell Signaling), anti-calponin 1/2/3 (for IF:sc-28545, FL-297, Santa Cruz Biotech), anti-CD31 (for IHC: #550274, BD Biosciences), anti-fibronectin (for IF, IHC and WB: ab-23750, Abcam), anti-mitochondria (for IF: MAB1273, Milllipore), anti-Beclin-1 (for IF: #2026-1, Epitomics), anti-LAMP-1 (for WB: sc-17768, Santa Cruz Biotech) and anti-LAMP-2 (for WB: sc-18822, Santa Cruz Biotech). Hoechst-33258 nuclear stain (Sigma). Other reagents

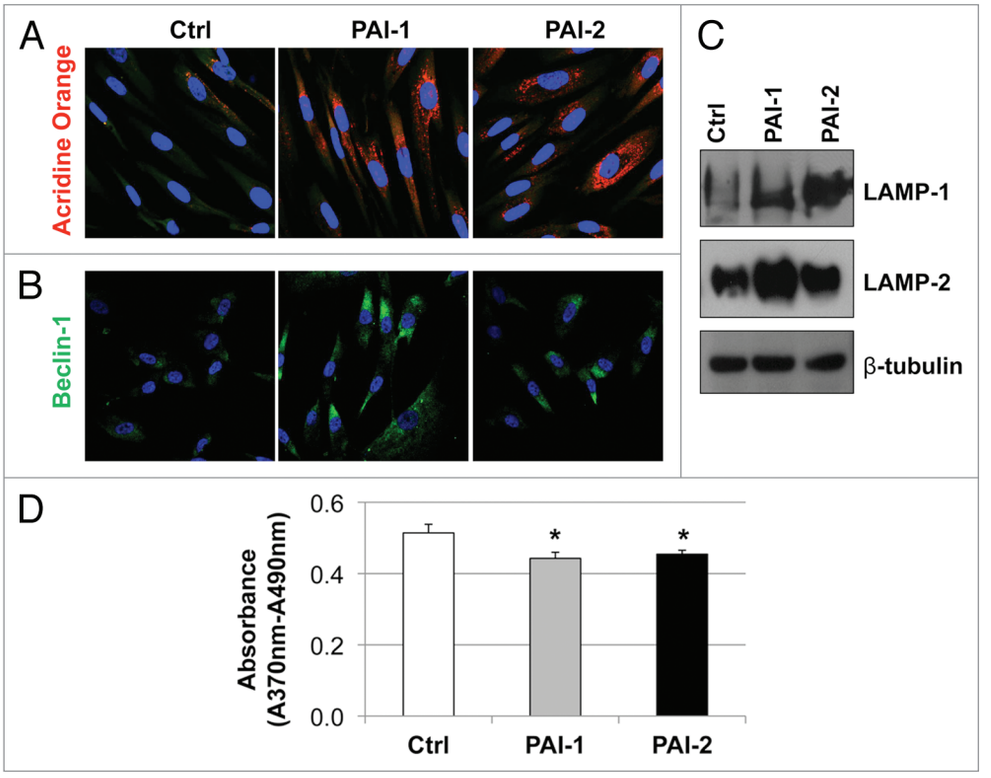

Figure 8. Recombinant expression of PAI-1 or PAI-2 increases autophagy in fibroblasts. To assess the effects of PAI-1 and PAI-2 overexpression on autophagy in fibroblasts, the levels of a variety of autophagic markers were assessed in control fibroblasts and in PAI-1/2(+)-overexpressing fibroblasts. (A) Determination of AVOs (acidic vesicular organelles) using acridine orange. In orange-acridine stained cells, cytoplasm fluorescences green, whereas acid compartments fluorescence red. Note that fibroblasts overexpressing PAI-1 or PAI-2 display a larger amount of AVOs compared with control fibroblasts. Images captured at original magnification of 63x. Nuclei were stained with Hoechst (blue). (B) Localization of Beclin-1. Note that overexpression of PAI-1 or PAI-2 upregulates the expression of Beclin-1, an autophagic marker. Images were captured at an original magnification of 63x. Nuclei were stained with Hoechst (blue). (C) Immunoblotting for LAMP-1 and LAMP-2. Note that the expression of autophagic markers, LAMP-1 and LAMP-2, is increased in fibroblasts overexpressing PAI-1 or PAI-2. Immunoblotting with β-tubulin is shown as a control for equal loading. (D) Proliferation of fibroblasts overexpressing PAI-1 or PAI-2. Note that BrdU incorporation is significantly reduced in fibroblasts overexpressing PAI-1 or PAI-2 as compared with control fibroblasts. Results are represented as the mean ± SEM. An asterisk indicates that $p \leq 0.05$, compared with controls. Ctrl, fibroblasts containing empty vector alone; PAI-1, fibroblasts overexpressing PAI-1; PAI-2, fibroblasts overexpressing PAI-2.

were as follows, Hoechst-33258 nuclear stain was from Sigma and Anti-fade reagent (S2828) was from Invitrogen.

Cell cultures. Human immortalized fibroblasts (hTERT-BJ1) and human GFP-positive breast cancer cells (MDA-MB-231-GFP) were grown in Dulbecco's modified Eagle medium (DMEM) containing 10% fetal bovine serum in a 37°C, 5% CO_2 incubator. MDA-MB-231 (GFP^+) cells were the generous gift of Dr. A. Fatatis (Drexel University, Philadelphia, PA).

Recombinant expression of PAI-1 and PAI-2. hTERT-BJ1 fibroblasts were transduced with a lentiviral vector encoding: PAI-1 (Plasminogen Activator Inhibitor type-1, Accession# NM_000602) with the construct pReceiver-F0606-Lv105, PAI-2 (Plasminogen Activator Inhibitor type-2, Accession# J02685) with the construct pReceiver-F0195-Lv105 or vector alone (pReceiver-Lv105) as a negative control (GeneCopoeia, Inc.). lentiviral vectors were transfected into the 293Ta lentiviral packaging cell line using Lenti-Pac HIV Expression Packaging Kit (GeneCopoeia), according to the manufacturer's instructions. After 48 h, virus-containing medium was passed through a 0.45 μm filter and added to hTERTBJ1 cells in the presence of 5 μg/ml Polybrene. Infected hTERT fibroblasts were selected in the presence of 1.5 μg/ml puromycin.

Isolation of mammary stromal fibroblasts. Primary mammary fibroblasts were isolated basically as previously described in reference 9. Briefly, the fourth and fifth mammary glands from 8-week-old virgin wild-type and Cav-$1^{-/-}$ mice were removed aseptically, minced with surgical blades, incubated in a shaker (for 2 to 3 h at 37°C) in 30 to 35 ml of digestion media (DMEM [Dulbecco's modified Eagle medium]) containing 2 mg/ml collagenase type I and 50 μg/ml gentamicin. Then, the cell suspensions were spun 10 min at 1,000 rpm to eliminate floating fat cells. Cell pellets were washed twice in 10 ml of growth media (DMEM, 10% fetal bovine serum, pen/strep) containing fungizone. Then, cell pellets were disaggregated by pipetting up and down 10 to 15 times with a sterile 1-ml blue pipette tip. Mammary fibroblasts were cultured in growth media containing fungizone for one week. Then, fibroblasts were grown and passaged in growth media.

Proteomic analysis. 2D DIGE (2-dimensional difference gel electrophoresis) [53] and mass spectrometry protein identification

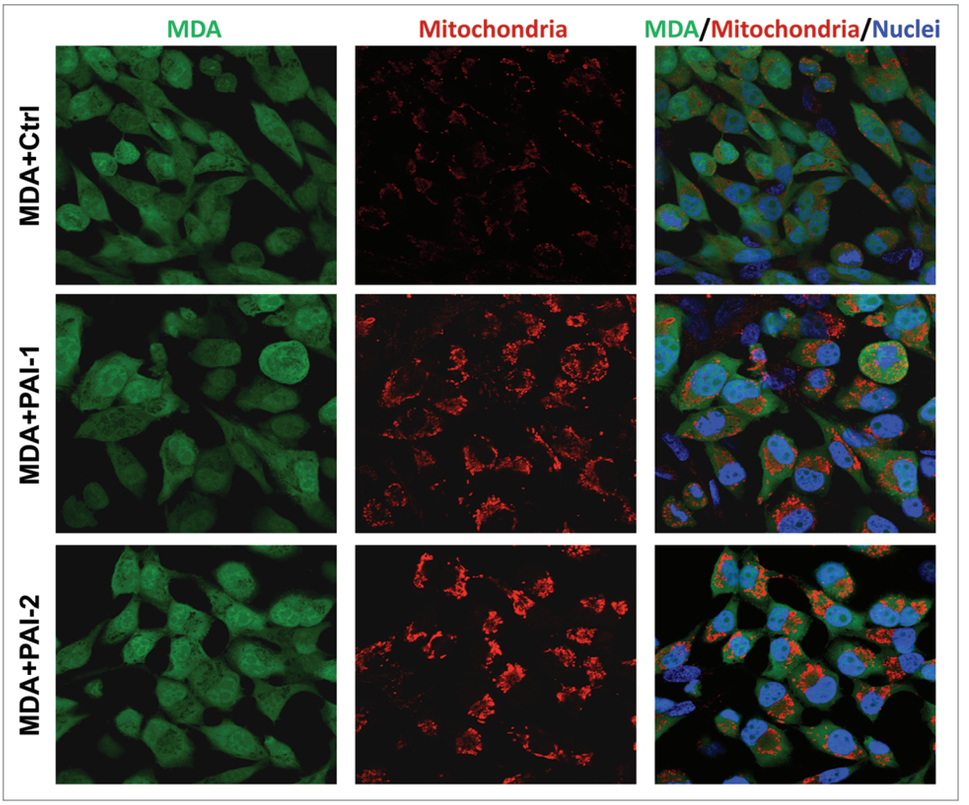

Figure 9. Fibroblasts overexpressing PAI-1 or PAI-2 increase the mitochondrial mass of adjacent breast cancer cells. Co-cultures of MDA-MB-231 cells and fibroblasts (control vs. those overexpressing PAI-1 or PAI-2) were immunostained with antibodies against a mitochondrial membrane antigen (red). Note that the mitochondrial mass is higher in MDA-MB-231 cells in co-culture with PAI-1/2(+) fibroblasts as compared with control fibroblasts. Hoechst was used to stain nuclei (blue). Images captured at an original magnification of 63x. Ctrl, fibroblasts containing empty vector alone; PAI-1, fibroblasts overexpressing PAI-1; PAI-2, fibroblasts overexpressing PAI-2.

were run by Applied Biomics (Hayward, CA). Image scans were performed immediately following the SDS-PAGE using Typhoon TRIO (Amersham BioSciences) following the protocols provided. The scanned images were then analyzed by Image QuantTL software (GE-Healthcare) and then subjected to in-gel analysis and cross-gel analysis using DeCyder software version 6.5 (GE-Healthcare). The ratio of protein differential expression was obtained from in-gel DeCyder software analysis. The selected spots were picked by an Ettan Spot Picker (GE-Healthcare) following the DeCyder software analysis and spot picking design. The selected protein spots were subjected to in-gel trypsin digestion, peptides extraction, desalting and followed by MALDI-TOF/TOF (Applied Biosystems) analysis to determine the protein identity.

Production of fibroblast-derived extracellular matrices. Fibroblast-derived extracellular matrices were prepared as previously described in reference 54–56. Briefly, wild-type and Cav-1 KO mammary stromal fibroblasts (between passages 3 and 6) were seeded at a density of 2.5 x 10^5 cells/ml onto chemically cross-linked, gelatin-coated tissue culture dishes. Once the fibroblasts reached confluence, fresh medium containing 50 μg/ml of ascorbic acid was added every 48 h for 5 d. After 5 d, unextracted matrices were immunostained with Hoechst and anti-fibronectin antibody, as described below.

Immunofluorescence. Unextracted extracellular matrices or fibroblasts grown on glass coverslips were washed three times with PBS containing Ca and Mg (PBS/CM). Then, extracellular matrices or cells were fixed with 2% PFA for 30 min and washed with PBS/CM. After fixation, cells were permeabilized using PBS/CM containing 0.1% Triton for 10 min, washed with PBS/CM and treated with 25 mmol/L NH_4Cl in PBS for 10 min to quench free aldehyde groups. Primary antibodies were added to each coverslips and incubated for 1 h at RT before addition of the appropriated fluorochrome-conjugated secondary antibodies for 30 min at RT. Finally, slides were washed, incubated with the nuclear stain (Hoechst) and mounted. Images were collected with a Zeiss LSM510 meta confocal system using a 405 nm Diode excitation laser with a band pass filter of 420–480 nm, a 488 nm Argon excitation laser with a band pass filter of 505–550 nm and a 543 nm HeNe excitation laser with a 561–604 nm filter.

Detection of acidic vesicular organelles (AVOs) with acridine orange. Autophagy is characterized by the formation and promotion of acidic vesicular organelles (AVOs). To detect AVOs in fibroblasts, we performed the vital staining with acridine orange. This reagent is a weak base that moves freely across biological membranes. When acridine orange is located in the cytoplasm, it fluoresces green, whereas in acidic compartments, it forms aggregates that fluoresce bright red.[38,39] Fibroblasts grown on glass coverslips in 12-well plates were washed PBS and incubated with acridine orange (Invitrogen) (1 μg/ml) for 15 min. After washing with PBS, cells were fixed with 4% Parafolmahedyde for 30 min at RT, counterstained with Hoechst and mounted.

Western blot analysis. Cell protein lysates were obtained by cell scraping with lysis buffer (10 mM Tris, pH 7.5, 150 mM NaCl, 1% Triton X-100 and 60 mM *n*-octyl-glucoside), containing protease inhibitors (Boehringer Mannheim, Indianapolis, IN). Samples were incubated on a rotating platform at 4°C and were then centrifuged at 12,000x g for 10 min (at 4°C) to remove insoluble debris. Protein concentrations were analyzed using the BCA reagent (Pierce, Rockford, IL). Samples were then separated by SDS-PAGE (10% acrylamide) and transferred to nitrocellulose. All subsequent wash buffers contained 10 mM Tris, pH 8.0,

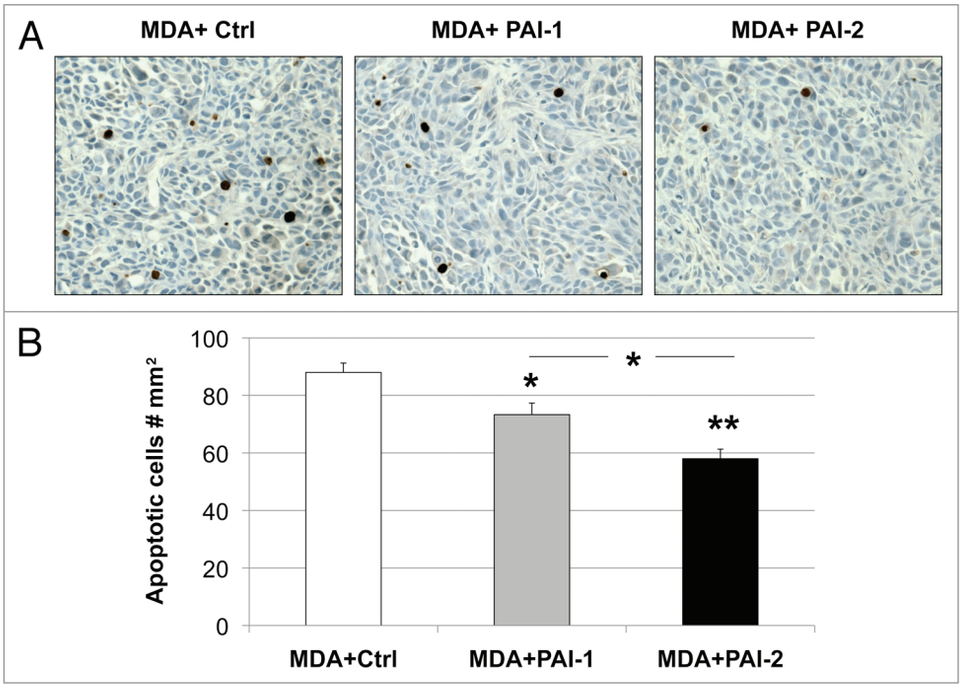

Figure 10. Overexpression of PAI-1 or PAI-2 in stromal fibroblasts reduces tumor apoptosis. Tunnel assays were performed on MDA-MB-231 tumors grown in the presence of fibroblasts (control vs. those overexpressing PAI-1 or PAI-2) and the numbers of apoptotic cells were quantitated. (A) Representative images of tunnel assay staining are shown. Images were captured at an original magnification of 40x. Slides were counterstained with hematoxylin. (B) Quantification of apoptotic tumor cell number. Note that apoptosis in MDA-MB-231 was significantly reduced when grown in presence of PAI-1- or PAI-2-overexpresing fibroblasts as compared with control fibroblasts. Results are represented as the mean ± SEM. An asterisk indicates that $p \leq 0.05$ and two asterisks indicate that $p \leq 0.001$. Ctrl, fibroblasts containing empty vector alone; PAI-1, fibroblasts overexpressing PAI-1; PAI-2, fibroblasts overexpressing PAI-2; MDA, MDA-MB-231 (GFP^+).

150 mM NaCl, 0.1% Tween 20, which was supplemented with 5% nonfat dry milk (Carnation) for the blocking solution and 1% bovine serum albumin (Sigma) for the antibody diluent. Horseradish peroxidase-conjugated secondary antibodies were used to visualize bound primary antibodies with an ECL detection kit (Pierce). (Pierce, Rockford, IL).

Proliferation. Cell proliferation was determined using a standard BrdU assay (Roche). The incorporation of a pyrimidine analog (BrdU) was determined in hTERT-BJ1 fibroblasts, as suggested by the manufacturer. Briefly, fibroblasts were trypsinized and plated in a 96-well plate at a density of 2,000 cells/well. After 48 h, BrdU was added to each well and incubated for 24 h at 37°C. The next day, the absorbance at 370 nm and 492 nm was measured on a plate reader (Tecan).

Co-cultivation of breast cancer cells and fibroblasts. To test the effect of stromal fibroblasts on the growth of the breast cancer epithelial cells, 1 x 10^3 tumor cells (MDA-MB-231 expressing GFP) and 5 x 10^3 fibroblasts (hTERT-BJ1) were seeded in a 12-well microplate in growth media (DMEM, 10% fetal bovine serum, pen/strep). The intensity of GFP fluorescence of the cells in co-cultivation was considered a measurement for the growth and was determined at the indicated days in a microplate-fluorometer (Thermo Fisher). The fluorescence was normalized to the first day to correct differences in initial cell attachment.

Animal studies. All animals were housed and maintained in a pathogen free environment/barrier facility at the Kimmel Cancer Center at Thomas Jefferson University under National Institutes of Health (NIH) guidelines. Mice were kept on a 12 h light/dark cycle with ad libitum access to chow and water. Approval for all animal protocols used for this study was reviewed and approved by the Institutional Animal Care and Use Committee (IACUC). Briefly, a mixture of tumor cells (MDA-MB-231 [GFP(+)]; 1 x 10^6 cells) plus hTERT-BJ1 fibroblasts (3 x 10^5 cells) in 100 μl of sterile PBS were co-injected into the flanks of athymic NCr nude mice (NCRNU; Taconic Farms; 6–8 weeks of age). Mice were then sacrificed at 3 weeks post-injection; tumors were excised to determine their weight and size using calipers. Tumor volume was calculated using the formula $(X^2Y)/2$, where X is the width and Y is the length.

Immunohistochemistry. Paraffin-embedded tumor sections (4–6 μm) were incubated at 55°C for 30 min, dewaxed with xylene and rehydrated through a graded series of ethanol. Antigen retrieval was performed in 10 mM sodium citrate, pH 6 for 10 min using a pressure cooker. After cooling, the sections were blocked with 3% hydrogen peroxide followed by incubation with 10% goat serum/PBS for 1 h at RT. Primary antibodies were incubated overnight at 4°C. Next day, slides were washed twice with PBS for 5 min each and incubated with the appropriated biotinylated antibodies (1:500, Vector Labs, Burlingame, CA) for 30 min at RT. Slides were then washed and incubated with streptavidin-horseradish peroxidase solution for 30 min at RT. Immunoreactivity was revealed using an ImmPACT

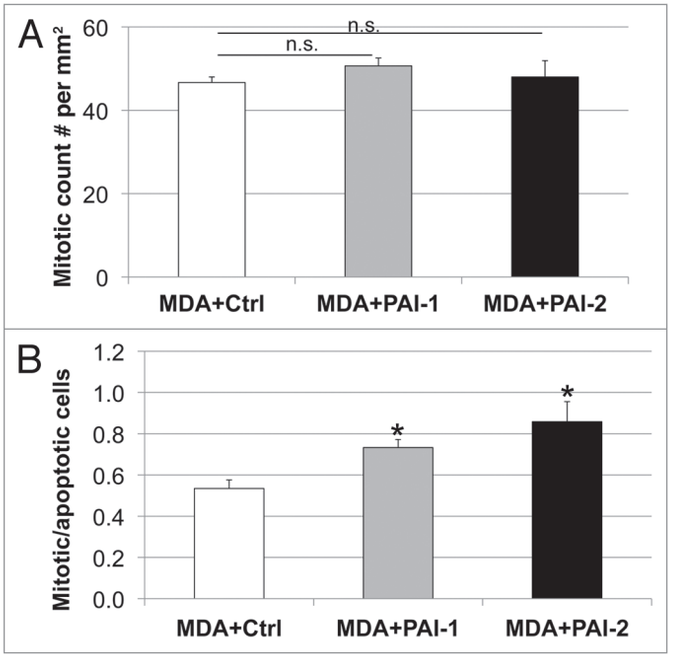

Figure 11. Fibroblasts overexpressing PAI-1 or PAI-2 do not affect the proliferation of tumor cells in vivo. (A) Quantification of mitotic tumor cells in MDA-MB-231 tumors grown in presence of control fibroblasts (Ctrl) or those overexpressing PAI-1 or PAI-2. Note that no significant differences were observed among these three groups. (B) Ratio of mitotic cells/apoptotic cells in epithelial tumor cells in MDA tumors grown in presence of fibroblasts. Note that the mitosis/apoptosis ratios are significantly higher for MDA tumors grown in the in presence of fibroblasts overexpressing PAI-1 or PAI-2 as compared with control fibroblasts. n.s.: not significant. Results are represented as the mean ± SEM. An asterisk indicates that $p \leq 0.05$ compared with controls. Ctrl, fibroblasts containing empty vector alone; PAI-1, fibroblasts overexpressing PAI-1; PAI-2, fibroblasts overexpressing PAI-2; MDA, MDA-MB-231 (GFP⁺).

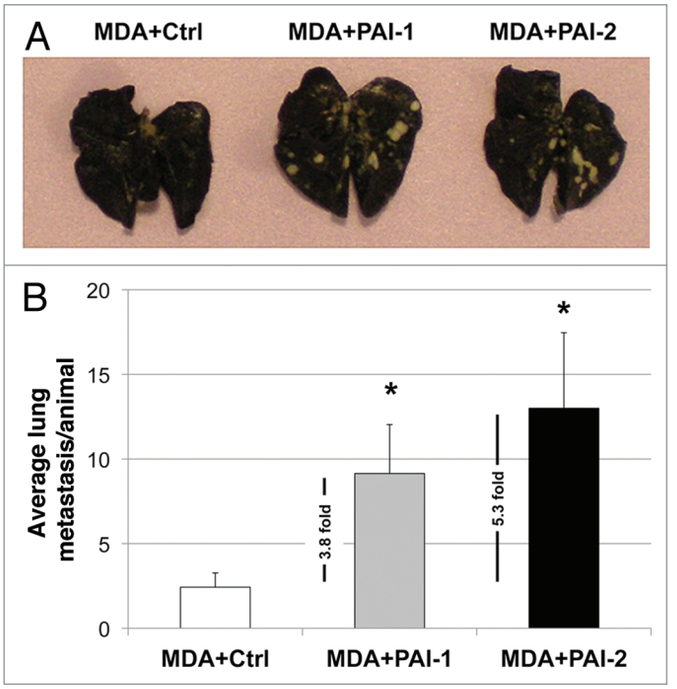

Figure 12. Fibroblasts overexpressing PAI-1 or PAI-2 increase lung metastasis. MDA-MB-231 cells were co-injected with fibroblasts in the tail vein of nude mice. After 7 weeks, the lungs were insufflated with India ink dye and the number of metastases was counted. (A) Representative images of lung metastasis for each group are shown. (B) Quantification of lung metastasis. Note that fibroblasts overexpressing PAI-1 or PAI-2 significantly increased the number of MDA-MB-231 lung metastases (~3.8 and 5.3 fold, respectively) as compared with controls. An asterisk indicates that $p \leq 0.05$. Ctrl, fibroblasts containing empty vector alone; PAI-1, fibroblasts overexpressing PAI-1; PAI-2, fibroblasts overexpressing PAI-2; MDA, MDA-MB-231 (GFP⁺).

NovaRED peroxidase substrate kit (Vector) per manufacturer's instructions. Finally, the sections were counterstained with hematoxylin for 5–10 sec, air-dried and mounted with coverslips. For quantification of tumor angiogenesis, CD31-positive vessels were enumerated in 4–6 fields within the central area of each tumor using a 20x objective lens and an ocular grid (0.25 mm^2 per field). The total numbers of vessel per unit area was calculated using Image J, and the data was represented graphically.

Quantification of tumor apoptosis. Apopototic cells were identified using the TUNEL-based ApopTag Peroxidase In Situ Apoptosis Detection Kit (Millipore, Temecula, CA) according to manufacturer's instructions. Briefly, paraffin sections were deparaffinized in xylene, rehydrated in ethanols and washed with PBS. The tissue sections were treated with 20 μg/ml proteinase K (Roche, Indianapolis, IN) diluted in PBS for 15 min at room temperature (RT), washed and blocked with 3% hydrogen peroxide for 5 min. The sections were then incubated with equilibration buffer briefly, followed by working strength TdT enzyme for 1 h at 37°C. After washing, the sections were incubated with anti-digoxigenin horseradish peroxidase conjugated antibody for 30 min at RT, washed, and apoptotic positive cells were detected using 3,3'-diaminobenzidine (Dako Products, Carpinteria, CA). Apoptotic cells were counted in 4–6 fields within the central area of each tumor using a 40x objective lens and an ocular grid (0.0625 mm^2 per field). The total numbers of vessel per unit area was calculated using Image J, and the data was represented graphically.

Experimental metastasis (lung colonization assay). For the metastasis study, a mixture of tumor cells (MDA-MB-231 [GFP(+)]; 4.5 x 10^5 cells) plus hTERT-BJ1 fibroblasts (1.5 x 10^5 cells) in 100 μl of sterile PBS were co-injected via the tail vein of athymic nude mice and divided in three groups. After 7 weeks of every-other-day intra-peritoneal injections, the lungs were removed and insuflated with 15% India Ink dye, washed in water and bleached in Fekete's solution (70% ethanol, 3.7% paraformaldehyde, 0.75 M glacial acetic acid). The number of lung colonies was determined using a low-power stereo microscope (Nikon SMZ-1500, Tokyo, Japan). p-values were determined by applying Mann-Whitney statistical analysis, which does not assume a Gaussian distribution (non-parametric test).

Acknowledgments

M.P.L. and his laboratory were supported by grants from the NIH/NCI (R01-CA-080250; R01-CA-098779;

R01-CA-120876; R01-AR-055660) and the Susan G. Komen Breast Cancer Foundation. A.K.W. was supported by a Young Investigator Award from Breast Cancer Alliance, Inc. and a Susan G. Komen Career Catalyst Grant. F.S. was supported by grants from the W.W. Smith Charitable Trust, the Breast Cancer Alliance (BCA) and a Research Scholar Grant from the American Cancer Society (ACS). Funds were also contributed by the Margaret Q. Landenberger Research Foundation (to M.P.L.). R.G.P. was supported by grants from the NIH/NCI (R01-CA-70896, R01-CA-75503, R01-CA-86072 and R01-CA-107382) and the Dr. Ralph and Marian C. Falk Medical Research Trust. The Kimmel Cancer Center was supported by the NIH/NCI Cancer Center Core grant P30-CA-56036 (to R.G.P.).

This project is funded, in part, under a grant with the Pennsylvania Department of Health (to M.P.L. and F.S.). The Department specifically disclaims responsibility for any analyses, interpretations or conclusions. This work was also supported, in part, by a Centre grant in Manchester from Breakthrough Breast Cancer in the UK (to A.H.) and an Advanced ERC Grant from the European Research Council.

References

1. Tlsty TD, Coussens LM. Tumor stroma and regulation of cancer development. Annu Rev Pathol 2006; 1:119-50; DOI: 10.1146/annurev.pathol.1.110304.100224.
2. Bissell MJ, Radisky D. Putting tumours in context. Nat Rev Cancer 2001; 1:46-54; DOI: 10.1038/35094059.
3. Rønnov-Jessen L, Bissell MJ. Breast cancer by proxy: can the microenvironment be both the cause and consequence? Trends Mol Med 2009; 15:5-13; DOI: 10.1016/j.molmed.2008.11.001.[L1]
4. Kalluri R, Zeisberg M. Fibroblasts in cancer. Nat Rev Cancer 2006; 6:392-401; DOI: 10.1038/nrc1877.
5. Orimo A, Weinberg RA. Stromal fibroblasts in cancer: a novel tumor-promoting cell type. Cell Cycle 2006; 5:1597-601; DOI: 10.4161/cc.5.15.3112.
6. Orimo A, Gupta PB, Sgroi DC, Arenzana-Seisdedos F, Delaunay T, Naeem R, et al. Stromal fibroblasts present in invasive human breast carcinomas promote tumor growth and angiogenesis through elevated SDF-1/CXCL12 secretion. Cell 2005; 121:335-48; DOI: 10.1016/j.cell.2005.02.034.
7. Hwang RF, Moore T, Arumugam T, Ramachandran V, Amos KD, Rivera A, et al. Cancer-associated stromal fibroblasts promote pancreatic tumor progression. Cancer Res 2008; 68:918-26; DOI: 10.1158/0008-5472.CAN-07-5714.
8. Mercier I, Casimiro MC, Wang C, Rosenberg AL, Quong J, Minkeu A, et al. Human breast cancer-associated fibroblasts (CAFs) show caveolin-1 downregulation and RB tumor suppressor functional inactivation: Implications for the response to hormonal therapy. Cancer Biol Ther 2008; 7:1212-25; DOI: 10.4161/cbt.7.8.6220.
9. Sotgia F, Del Galdo F, Casimiro MC, Bonuccelli G, Mercier I, Whitaker-Menezes D, et al. Caveolin-1$^{-/-}$ null mammary stromal fibroblasts share characteristics with human breast cancer-associated fibroblasts. Am J Pathol 2009; 174:746-61; DOI: 10.2353/ajpath.2009.080658.
10. Pavlides S, Whitaker-Menezes D, Castello-Cros R, Flomenberg N, Witkiewicz AK, Frank PG, et al. The reverse Warburg effect: aerobic glycolysis in cancer-associated fibroblasts and the tumor stroma. Cell Cycle 2009; 8:3984-4001; DOI: 10.4161/cc.8.23.10238.
11. Williams TM, Sotgia F, Lee H, Hassan G, Di Vizio D, Bonuccelli G, et al. Stromal and epithelial caveolin-1 both confer a protective effect against mammary hyperplasia and tumorigenesis: Caveolin-1 antagonizes cyclin D1 function in mammary epithelial cells. Am J Pathol 2006; 169:1784-801; DOI: 10.2353/ajpath.2006.060590.
12. Trimmer C, Sotgia F, Whitaker-Menezes D, Balliet R, Eaton G, Martinez-Outschoorn UE, et al. Caveolin-1 and mitochondrial SOD2 (MnSOD) function as tumor suppressors in the stromal microenvironment: A new genetically tractable model for human cancer-associated fibroblasts. Cancer Biol Ther 2011; 11:383-94; DOI: 10.4161/cbt.11.4.14101.
13. Witkiewicz AK, Casimiro MC, Dasgupta A, Mercier I, Wang C, Bonuccelli G, et al. Towards a new "stromal-based" classification system for human breast cancer prognosis and therapy. Cell Cycle 2009; 8:1654-8; DOI: 10.4161/cc.8.11.8544.
14. Witkiewicz AK, Dasgupta A, Nguyen KH, Liu C, Kovatich AJ, Schwartz GF, et al. Stromal caveolin-1 levels predict early DCIS progression to invasive breast cancer. Cancer Biol Ther 2009; 8:1071-9; DOI: 10.4161/cbt.8.11.8874.
15. Witkiewicz AK, Dasgupta A, Sammons S, Er O, Potoczek MB, Guiles F, et al. Loss of stromal caveolin-1 expression predicts poor clinical outcome in triple negative and basal-like breast cancers. Cancer Biol Ther 2010; 10:135-43; DOI: 10.4161/cbt.10.2.11983.
16. Witkiewicz AK, Dasgupta A, Sotgia F, Mercier I, Pestell RG, Sabel M, et al. An absence of stromal caveolin-1 expression predicts early tumor recurrence and poor clinical outcome in human breast cancers. Am J Pathol 2009; 174:2023-34; DOI: 10.2353/ajpath.2009.080873.
17. Sloan EK, Ciocca DR, Pouliot N, Natoli A, Restall C, Henderson MA, et al. Stromal cell expression of caveolin-1 predicts outcome in breast cancer. Am J Pathol 2009; 174:2035-43; DOI: 10.2353/ajpath.2009.080924.
18. Di Vizio D, Morello M, Sotgia F, Pestell RG, Freeman MR, Lisanti MP. An absence of stromal caveolin-1 is associated with advanced prostate cancer, metastatic disease and epithelial Akt activation. Cell Cycle 2009; 8:2420-4; DOI: 10.4161/cc.8.15.9116.
19. Pavlides S, Tsirigos A, Migneco G, Whitaker-Menezes D, Chiavarina B, Flomenberg N, et al. The autophagic tumor stroma model of cancer: Role of oxidative stress and ketone production in fueling tumor cell metabolism. Cell Cycle 2010; 9:3485-505; DOI: 10.4161/cc.9.17.12721.
20. Martinez-Outschoorn UE, Whitaker-Menezes D, Pavlides S, Chiavarina B, Bonuccelli G, Casey T, et al. The autophagic tumor stroma model of cancer or "battery-operated tumor growth": A simple solution to the autophagy paradox. Cell Cycle 2010; 9:4297-306; DOI: 10.4161/cc.9.21.13817.
21. Chiavarina B, Whitaker-Menezes D, Migneco G, Martinez-Outschoorn UE, Pavlides S, Howell A, et al. HIF-1alpha functions as a tumor promoter in cancer-associated fibroblasts and as a tumor suppressor in breast cancer cells: Autophagy drives compartment-specific oncogenesis. Cell Cycle 2010; 9:3534-51; DOI: 10.4161/cc.9.17.12908.
22. Martinez-Outschoorn UE, Trimmer C, Lin Z, Whitaker-Menezes D, Chiavarina B, Zhou J, et al. Autophagy in cancer-associated fibroblasts promotes tumor cell survival: Role of hypoxia, HIF1 induction and NFkappaB activation in the tumor stromal microenvironment. Cell Cycle 2010; 9:3515-33; DOI: 10.4161/cc.9.17.12928.
23. Lisanti MP, Martinez-Outschoorn UE, Chiavarina B, Pavlides S, Whitaker-Menezes D, Tsirigos A, et al. Understanding the "lethal" drivers of tumor-stroma co-evolution: emerging role(s) for hypoxia, oxidative stress and autophagy/mitophagy in the tumor microenvironment. Cancer Biol Ther 2010; 10:537-42; DOI: 10.4161/cbt.10.6.13370.
24. Duffy MJ. The urokinase plasminogen activator system: role in malignancy. Curr Pharm Des 2004; 10:39-49; DOI: 10.2174/1381612043453559.
25. Andreasen PA, Georg B, Lund LR, Riccio A, Stacey SN. Plasminogen activator inhibitors: hormonally regulated serpins. Mol Cell Endocrinol 1990; 68:1-19; DOI: 10.1016/0303-7207(90)90164-4.
26. Harbeck N, Kates RE, Gauger K, Willems A, Kiechle M, Magdolen V, et al. Urokinase-type plasminogen activator (uPA) and its inhibitor PAI-I: novel tumor-derived factors with a high prognostic and predictive impact in breast cancer. Thromb Haemost 2004; 91:450-6;.
27. Look MP, van Putten WLJ, Duffy MJ, Harbeck N, Christensen IJ, Thomssen C, et al. Pooled Analysis of Prognostic Impact of Urokinase-Type Plasminogen Activator and Its Inhibitor PAI-1 in 8377 Breast Cancer Patients. J Natl Cancer Inst 2002; 94:116-28;.
28. Castelló R, Estelles A, Vazquez C, Falco C, Espana F, Almenar SM, et al. Quantitative real-time reverse transcription-PCR assay for urokinase plasminogen activator, plasminogen activator inhibitor type 1 and tissue metalloproteinase inhibitor type 1 gene expressions in primary breast cancer. Clin Chem 2002; 48:1288-95;.
29. Foekens JA, Peters HA, Look MP, Portengen H, Schmitt M, Kramer MD, et al. The urokinase system of plasminogen activation and prognosis in 2,780 breast cancer patients. Cancer Res 2000; 60:636-43;.
30. Duffy MJ, Duggan C. The urokinase plasminogen activator system: a rich source of tumour markers for the individualised management of patients with cancer. Clin Biochem 2004; 37:541-8; DOI: 10.1016/j.clinbiochem.2004.05.013.
31. Croucher DR, Saunders DN, Lobov S, Ranson M. Revisiting the biological roles of PAI2 (SERPINB2) in cancer. Nat Rev Cancer 2008; 8:535-45; DOI: 10.1038/nrc2400.
32. Duffy MJ. Urokinase plasminogen activator and its inhibitor, PAI-1, as prognostic markers in breast cancer: from pilot to level 1 evidence studies. Clin Chem 2002; 48:1194-7;.
33. Umeda T, Eguchi Y, Okino K, Kodama M, Hattori T. Cellular localization of urokinase-type plasminogen activator, its inhibitors, and their mRNAs in breast cancer tissues. J Pathol 1997; 183:388-97; DOI: 10.1002/(SICI)1096-9896(199712)183:4<388::AID-PATH943>3.0.CO;2-I.
34. Offersen BV, Nielsen BS, Hoyer-Hansen G, Rank F, Hamilton-Dutoit S, Overgaard J, et al. The myofibroblast is the predominant plasminogen activator inhibitor-1-expressing cell type in human breast carcinomas. Am J Pathol 2003; 163:1887-99; DOI: 10.1016/S0002-9440(10)63547-X.
35. Sadlonova A, Bowe DB, Novak Z, Mukherjee S, Duncan VE, Page GP, et al. Identification of molecular distinctions between normal breast-associated fibroblasts and breast cancer-associated fibroblasts. Cancer Microenviron 2009; 2:9-21; DOI: 10.1007/s12307-008-0017-0.
36. Dublin E, Hanby A, Patel NK, Liebman R, Barnes D. Immunohistochemical expression of uPA, uPAR and PAI-1 in breast carcinoma. Fibroblastic expression has strong associations with tumor pathology. Am J Pathol 2000; 157:1219-27; DOI: 10.1016/S0002-9440(10)64637-8.

37. Martinez-Outschoorn UE, Pavlides S, Whitaker-Menezes D, Daumer KM, Milliman JN, Chiavarina B, et al. Tumor cells induce the cancer-associated fibroblast phenotype via caveolin-1 degradation: Implications for breast cancer and DCIS therapy with autophagy inhibitors. Cell Cycle 2010; 9:2423-33; DOI: 10.4161/cc.9.12.12048.
38. Arvan P, Rudnick G, Castle JD. Osmotic properties and internal pH of isolated rat parotid secretory granules. J Biol Chem 1984; 259:13567-72;.
39. Mains RE, May V. The role of a low pH intracellular compartment in the processing, storage and secretion of ACTH and endorphin. J Biol Chem 1988; 263:7887-94;.
40. Lee EK, Lee YS, Han IO, Park SH. Expression of Caveolin-1 reduces cellular responses to TGFbeta1 through downregulating the expression of TGFbeta type II receptor gene in NIH3T3 fibroblast cells. Biochem Biophys Res Commun 2007; 359:385-90; DOI: 10.1016/j.bbrc.2007.05.121.
41. Bonuccelli G, Whitaker-Menezes D, Castello-Cros R, Pavlides S, Pestell RG, Fatatis A, et al. The reverse Warburg effect: glycolysis inhibitors prevent the tumor promoting effects of caveolin-1 deficient cancer-associated fibroblasts. Cell Cycle 2010; 9:1960-71; DOI: 10.4161/cc.9.10.11601.
42. Kietzmann T, Roth U, Jungermann K. Induction of the plasminogen activator inhibitor-1 gene expression by mild hypoxia via a hypoxia response element binding the hypoxia-inducible factor-1 in rat hepatocytes. Blood 1999; 94:4177-85;.
43. Chen Y, Kong J, Sun T, Li G, Szeto FL, Liu W, et al. 1,25-Dihydroxyvitamin D3 suppresses inflammation-induced expression of plasminogen activator inhibitor-1 by blocking nuclear factor-[kappa]B activation. Arch Biochem Biophys 2011; 507:241-7; DOI: 10.1016/j.abb.2010.12.020.
44. Kruithof EK, Baker MS, Bunn CL. Biological and clinical aspects of plasminogen activator inhibitor type 2. Blood 1995; 86:4007-24;.
45. Pavlides S, Tsirigos A, Vera I, Flomenberg N, Frank PG, Casimiro MC, et al. Loss of stromal caveolin-1 leads to oxidative stress, mimics hypoxia and drives inflammation in the tumor microenvironment, conferring the "reverse Warburg effect": A transcriptional informatics analysis with validation. Cell Cycle 2010; 9:2201-19; DOI: 10.4161/cc.9.11.11848.
46. Martinez-Outschoorn UE, Balliet RM, Rivadeneira DB, Chiavarina B, Pavlides S, Wang C, et al. Oxidative stress in cancer-associated fibroblasts drives tumor-stroma co-evolution: A new paradigm for understanding tumor metabolism, the field effect and genomic instability in cancer cells. Cell Cycle 2010; 9:3256-76; DOI: 10.4161/cc.9.16.12553.
47. Bonuccelli G, Tsirigos A, Whitaker-Menezes D, Pavlides S, Pestell RG, Chiavarina B, et al. Ketones and lactate "fuel" tumor growth and metastasis: Evidence that epithelial cancer cells use oxidative mitochondrial metabolism. Cell Cycle 2010; 9:3506-14; DOI: 10.4161/cc.9.17.12731.
48. Alizadeh H, Ma D, Berman M, Bellingham D, Comerford SA, Gething MJ, et al. Tissue-type plasminogen activator-induced invasion and metastasis of murine melanomas. Curr Eye Res 1995; 14:449-58; DOI: 10.3109/02713689509003755.
49. Soff GA, Sanderowitz J, Gately S, Verrusio E, Weiss I, Brem S, et al. Expression of plasminogen activator inhibitor type 1 by human prostate carcinoma cells inhibits primary tumor growth, tumor-associated angiogenesis and metastasis to lung and liver in an athymic mouse model. J Clin Invest 1995; 96:2593-600; DOI: 10.1172/JCI118323.
50. Singh H, Dang TD, Ayala GE, Rowley DR. Transforming growth factor-beta1 induced myofibroblasts regulate LNCaP cell death. J Urol 2004; 172:2421-5; DOI: 10.1097/01.ju.0000138082.68045.48.
51. Razani B, Zhang XL, Bitzer M, von Gersdorff G, Bottinger EP, Lisanti MP. Caveolin-1 regulates transforming growth factor (TGF)beta/SMAD signaling through an interaction with the TGFbeta type I receptor. J Biol Chem 2001; 276:6727-38; DOI: 10.1074/jbc.M008340200.
52. Westerhausen DR Jr, Hopkins WE, Billadello JJ. Multiple transforming growth factor-beta-inducible elements regulate expression of the plasminogen activator inhibitor type-1 gene in Hep G_2 cells. J Biol Chem 1991; 266:1092-100;.
53. Marouga R, David S, Hawkins E. The development of the DIGE system: 2D fluorescence difference gel analysis technology. Anal Bioanal Chem 2005; 382:669-78; DOI: 10.1007/s00216-005-3126-3.
54. Castelló-Cros R, Cukierman E. Stromagenesis During Tumorigenesis: Characterization of Tumor-associated Fibroblasts and Stroma-derived 3D Matrices. Methods Mol Biol 2009; 522:275-305; DOI: 10.1007/978-1-59745-413-1_19.
55. Beacham DA, Amatangelo MD, Cukierman E. Preparation of extracellular matrices produced by cultured and primary fibroblasts. Curr Protoc Cell Biol 2007; 10:9.
56. Amatangelo MD, Bassi DE, Klein-Szanto AJ, Cukierman E. Stroma-derived three-dimensional matrices are necessary and sufficient to promote desmoplastic differentiation of normal fibroblasts. Am J Pathol 2005; 167:475-88; DOI: 10.1016/S0002-9440(10)62991-4.